

## High-pressure suppression of crystallization in the metallic supercooled liquid $Zr_{41}Ti_{14}Cu_{12.5}Ni_{10}Be_{22.5}$ : Influence of viscosity

W. H. Wang,<sup>1,\*</sup> Z. X. Wang,<sup>1</sup> D. Q. Zhao,<sup>1</sup> M. B. Tang,<sup>1</sup> W. Utsumi,<sup>2</sup> and X.-L. Wang<sup>3</sup>

<sup>1</sup>*Institute of Physics, Chinese Academy of Sciences, Beijing 100080, China*

<sup>2</sup>*Japan Atomic Energy Research Institute, SPring-8, Hyogo 679-5198, Japan*

<sup>3</sup>*Spallation Neutron Source and Metals Ceramics Division, Oak Ridge National Laboratory, Oak Ridge, Tennessee 37830, USA*

(Received 3 May 2004; published 17 September 2004)

The supercooled liquid  $Zr_{41}Ti_{14}Cu_{12.5}Ni_{10}Be_{22.5}$  is studied using a high-pressure (HP) and high-temperature x-ray diffraction technique with synchrotron radiation, which allows us for the first time to *in situ* monitor the crystallization kinetics of metallic supercooled liquid in both cooling and heating processes under HP. We find that more than 6 GPa can completely suppress the crystallization in the melt at low cooling rate, and distinct crystallization from glassy to melt states during fast heating can be bypassed at 8.3 GPa. HP suppresses the crystallization in the supercooled liquid through increasing its viscosity.

DOI: 10.1103/PhysRevB.70.092203

PACS number(s): 61.43.Fs, 62.50.+p, 64.70.Dv, 81.20.-n

The supercooled liquid (SL) with a metastable thermodynamic stability has remained one of the most inquisitive but obscure subjects of recent scientific interest.<sup>1-3</sup> Metallic liquid have often been regarded as ideal model systems of dense random packing, but it is unfortunate that rare metallic SLs are found to exist easily by a change in pressure and/or temperature. The recent developed bulk metallic glass (BMG) forming alloys are found to have particular stable SL state against crystallization, which offers a large experimentally accessible time and temperature windows for investigating the nature of the SL (Refs. 4 and 5) and for understanding the longstanding issues of nucleation, which is the key to control over crystallization and to develop new glassy and nanocrystalline materials with a unique combination of properties and manufacturability for applications.<sup>6-8</sup>

The BMG-forming liquid  $Zr_{41}Ti_{14}Cu_{12.5}Ni_{10}Be_{22.5}$  (vit1) is a relative strong liquid and exhibits a large viscosity (about 2.5 Pa s) around the melting point and large activation energy for flow.<sup>9,10</sup> This contrasts with most pure metals and alloys which are considered fragile liquids with much lower viscosities at melting point of  $10^{-3}$  Pa s and activation energy of 0.5 eV.<sup>11</sup> The stability of the SLs is found strongly depends on the treatment process and a pronounced asymmetry exists in crystallization behavior during constant heating and cooling of BMGs.<sup>8,12,13</sup> Differential scanning calorimetry (DSC) results shows that its crystallization temperature of vit1,  $T_x$  shifts to higher temperature with increasing heating rate,  $\phi$  and follows a linear relationship:  $T_x = 664.9 + 20.7 \ln \phi$ .<sup>14</sup> Assuming that the melting temperature of the alloy is independent of  $\phi$  and  $T_x$  continues to scale with  $\phi$ , the corresponding value of  $\phi$  for vit1 heated through the entire SL region into the equilibrium melt state without intervening of crystallization is about  $10^7$  K/s. In contrast, a rate of about 10 K/s is sufficient to suppress crystallization in the SL of vit1 and get full amorphous phase in cooling process.<sup>10</sup> These nucleation features lead to the excellent glass-forming ability, high thermal stability of the SL, controllable nanocrystallization and some interesting crystallization behaviors in the alloy.<sup>4-8,12</sup>

High pressure (HP) has been found to be a powerful tool for affecting and controlling the crystallization in the metal-

lic glasses.<sup>15,16</sup> Because both the nucleation and growth rates of crystalline phases in the glass-forming alloys strongly depend on the kinetics which is susceptible to pressure, the information on pressure affect on the crystallization is critical for gaining insight into the mechanism of the nucleation and glass formation in the BMG-forming SLs. However, little work on *in situ* HP crystallization has been conducted perhaps due to the experimental condition restrictions. This leaves many unresolved questions in this field. In this paper, we chose the representative SL, vit1, to study the effects of HP on crystallization during rapid cooling and heating process using a HP energy-dispersive x-ray diffraction (XRD) technique with synchrotron radiation, at a third-generation synchrotron radiation facility at Spring-8 in Japan.<sup>15</sup> The technique allows us for the first time to *in situ* monitor the crystallization kinetics of SL in both cooling and heating processes under HP. We show that HP can further stabilize the SL state and effectively suppress the crystallization of SL in cooling and even heating processes. The pronounced asymmetry behavior in crystallization during constant heating and cooling at ambient condition can be constricted under HP. Our results are likely to be important for understanding the nucleation mechanism of the BMGs.

Vit1 alloy was prepared by cast the melting alloy in a water-cooling Cu mould.<sup>13,14</sup> The  $T_g$ ,  $T_x$ , and liquidus temperature,  $T_l$  determined by DSC at a heating rate of 0.33 K/s at ambient pressure are 623, 693, and 1026 K, respectively.<sup>14</sup> The cooling and heating of the alloy were investigated by an *in situ* XRD technique at Spring-8 in Japan.<sup>17</sup> High-pressure and high-temperature conditions were generated using a cubic-type multi-anvil press (SMAP 180), and the sample assembly was similar to that used in Ref. 17. NiCr-NiAl thermocouple was brought into the pressurized zone and near the sample. NaCl powder was used as pressure transmitting medium, and the pressure was calibrated from its lattice constant with the accuracy about  $\pm 0.2$  GPa. The apparatus was designed to permit maximum heating rates of 150 K/s which cannot be realized in conventional thermal analyzers.<sup>17</sup> The pressure in the heating process was calibrated; pressure change is about 0.2–1 GPa during the heating process.<sup>17</sup> For

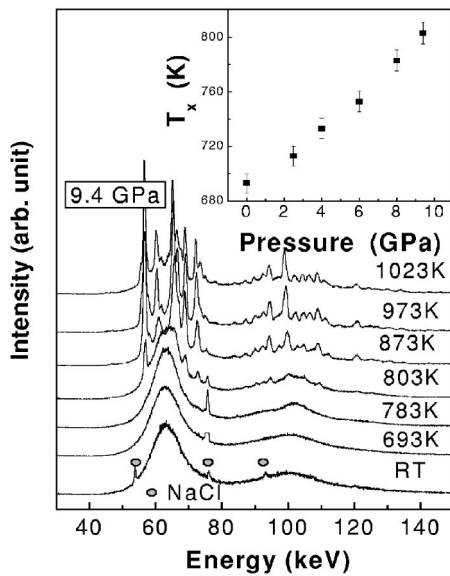


FIG. 1. *In situ* synchrotron XRD patterns of the  $Zr_{41}Ti_{14}Cu_{14.5}Ni_{10}Be_{22.5}$  BMG at elevating temperature under 9.4 GPa. The  $T_x$  increases from 693 K at ambient pressure to 803 K at 9.4 GPa. The inset shows the onset crystallization temperature of the vit1 upon pressure.  $T_x$  increases with increasing pressure with  $dT_x/dP=11.8$  K/GPa.

the HP rapid heating, the sample was rapidly heated from 693 K to above  $T_m$  with a heating rate of 40 K/s. The diffraction pattern was *in situ* recorded during the whole rapid heating process. For the cooling, the sample was first pressurized to high pressure, and then heated to 1373 K and kept for about 2 min. Then the heating electrical current was switched off and the sample was naturally cooled under HP. An energy dispersive method was utilized using white x-ray with energies of 20–150 keV. The diffracted x-ray was detected by a solid state Ge detector, at a diffraction angle  $2\theta=5^\circ$ .

Figure 1 shows XRD patterns of vit1 measured *in situ* at various temperatures under 9.4 GPa. The patterns were recorded every 5 K to determine the  $T_x$  and  $T_l$ . The time that the sample was kept at each temperature is about 30 s. Up to 783 K, the amorphous state is retained without a clear indication of crystallization within the limit of XRD measurement. The BMG starts to crystallize at about 803 K, 110 K above  $T_x$  at ambient pressure, indicating that  $T_x$  is increased to about 803 K under 9.4 GPa. The alloy is melted at about 1050 K and its value of  $T_l$  is not significantly changed under HP. The crystallization of vit1 is studied under various pressures, and the  $T_x$  shows significantly increase with increasing pressure as shown in the inset of Fig. 1. The  $dT_x/dP$  is about 11.8 K/GPa. The result implies that the  $T_x$  is susceptible to HP, and HP could be used to suppress crystallization when vit1 is heated. The increased activation energy barrier under pressure for diffusion makes the atomic redistribution on a large-range scale more difficult and the subsequent growth of the nuclei is inhibited. This results in the higher thermal stability of the SL under HP.<sup>16,18,19</sup>

Figure 2(a) shows *in situ* XRD patterns of vit1 in the rapid heating process at 8.3 GPa. In the HP rapid heating, the

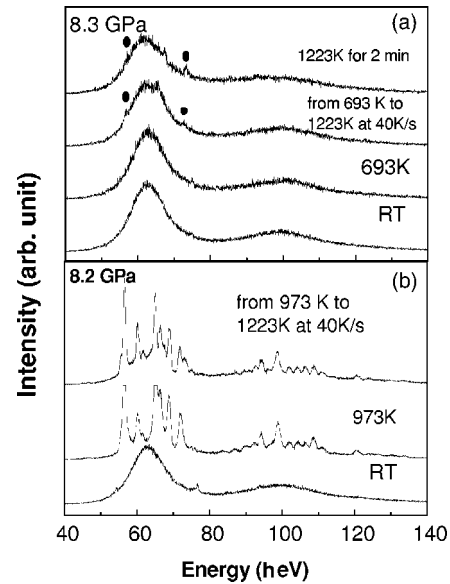


FIG. 2. (a) XRD patterns of vit1 alloy heated from supercooled liquid state to melt state with different heating rates. (●) marked the little nanocrystalline precipitation. (b) XRD patterns of crystalline vit1 (after full crystallization) heated to melt state with a heating rate of 40 K/s.

sample was firstly increased to 693 K which is much lower than  $T_x$  ( $T_x=783$  K at 8.3 GPa), and then, the sample was rapidly heated from 693 to 1223 K with a heating rate of 40 K/s. The diffracted x-ray pattern which was *in situ* recorded during the whole heating process shows that the alloy almost keeps in glassy state. Two weak broad peaks marked in Fig. 2(a) are from the precipitation of little fraction of nanocrystalline phase. The results indicate that no distinct crystallization is observed upon heating for glassy vit1 with a rate of 40 K/s, and the most amorphous phase is heated through the entire SL regime into the equilibrium melt without crystallization. In contrast, the crystallization event will occur when vit1 is heated with lower heating rates as shown in Fig. 1. To check if there is heating hysteresis effect in the rapid heating process, the sample was kept at 1223 K for 2 min. The XRD pattern shown in Fig. 1(a) is similar with that of the rapid heating alloy demonstrating no obvious heating hysteresis. We also rapid heated the fully crystallized vit1 from 973 to 1223 K with the same heating rate of 40 K/s, the XRD pattern in Fig. 2(b) shows that the crystallized phases can be mostly kept to 1223 K. This result means that if there is crystalline phases form during the rapid heating process, they cannot be melted during so rapid heating process, and confirms that rapid HP heating inhibits mostly the crystallization events when the BMG goes through SL to melt state.

The HP cooling process of vit1 is shown in Fig. 3(a). After vit1 is quenched from 1373 K to 300 K at 8.5 GPa with a estimated cooling rate of about 1 K/s, the samples show a broad scattering peak indicating the formation of full amorphous phase. The XRD traces for the alloy cooled at the same cooling rate under different pressures are presented in Fig. 3(b). The samples quenched with higher applied pressure ( $\geq 6$  GPa) show a full amorphous phase. When quench-

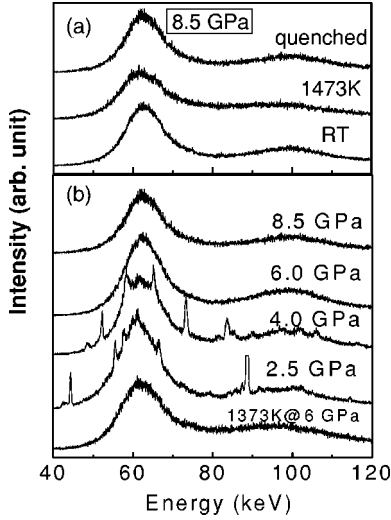


FIG. 3. (a) XRD patterns of the vit 1 melt cooled from equilibrium melt state to solid state at room temperature under 8.3 GPa. (b) XRD patterns of vit1 alloy cooled from equilibrium melt state to solid state at room temperature with the same cooling rate under various pressures.

ing pressure is lower than 4.5 GPa, there are few weak sharp crystalline peaks superimposing on the broad peak meaning that fully amorphization cannot be reached. The sample cooled with a similar cooling rate at ambient pressure consists of mostly the crystalline phases,<sup>20</sup> because the sample in the HP setup was covered with thick pyrophyllite and  $ZrO_2$  which have low thermal conductivity and solidified with much low cooling rate compared with that of cast in water-cooling Cu-mould. Furthermore, the covering materials also provide frequent abundance of sites that catalyze the nucleation of crystalline phase. The HP quenching result indicates that HP is effective to enhance glass formation by suppressing the crystallization in SL state of vit1.

To discuss above results, we use approach of classical nucleation serving as a simplified model. The steady state nucleation rate:<sup>21</sup>

$$I = AD \exp\left[-\frac{\Delta G^*}{kT}\right],$$

where  $A$  is constant,  $k$  is Boltzmann constant,  $T$  the absolute temperature, and  $D$  is effective diffusivity which is assumed to follow Arrhenius form,

$$D = D_0 \exp\left[-\frac{Q}{kT}\right],$$

here,  $D_0$  is pre-exponential factor,  $Q$  is diffusion activation energy,  $\Delta G^*$ , the activation energy for formation of stable nuclei is<sup>21</sup>

$$\Delta G^* = \frac{16\pi\sigma^3}{3(\Delta G)^2},$$

where  $\sigma$  and  $\Delta G$  are interfacial energy and free energy difference between the nuclei and liquid phase, respectively. We estimated  $\Delta G$  based on the DSC results in Ref. 22. Assuming

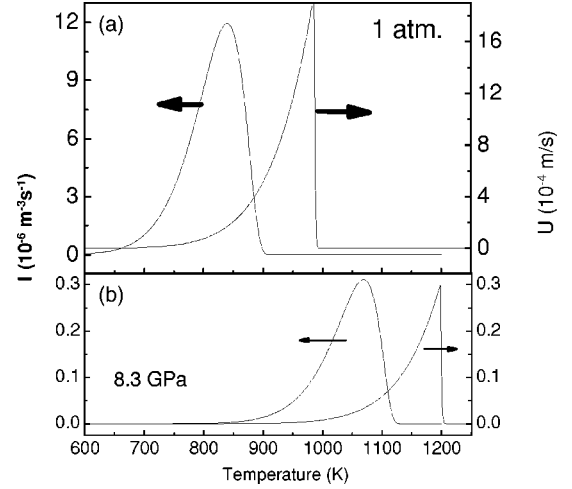


FIG. 4. The calculated temperature-dependent nucleation rate and growth rate of vit1 under ambient (a) and high pressure of 8.3 GPa (b).

diffusion-limited growth, the crystalline growth rate can be expressed by:<sup>23</sup>

$$U = \frac{D}{a} \left[ 1 - \exp\left(-\frac{\Delta G}{kT}\right) \right]$$

with the interatomic spacing  $a$ . Because  $\sigma$  is not sensitive to pressure compared to that of  $\Delta G$ , and the pressure effect on  $\Delta G^*$  and diffusion can be respectively expressed as

$$\left(\frac{\partial(\Delta G^*)}{\partial P}\right) = -\frac{32\pi\sigma^3}{3} \frac{\Delta V}{(\Delta G)^3},$$

$$\left(\frac{\partial(\ln D)}{\partial P}\right)_T = -\frac{\Delta V^*}{kT},$$

here  $\Delta V$  is the molar volume difference between the liquid and crystalline phases.  $\Delta V^*$  is activation volume. Therefore, under HP the steady state nucleation rate is

$$I_{HP} = AD_0 \exp\left[-\frac{Q + P\Delta V^* + \Delta G_P^*}{kT}\right] \quad (1)$$

here,

$$\Delta G_P^* = \frac{16\pi\sigma^3}{3(\Delta G + P\Delta V)^2}.$$

The growth velocity under HP,

$$U_{HP} = \frac{D_0}{a} \exp\left[-\frac{Q + P\Delta V^*}{kT}\right] \left[ 1 - \exp\left(-\frac{\Delta G + P\Delta V}{kT}\right) \right]. \quad (2)$$

For vit1,  $\sigma = 0.04$  J/m and  $A = 10$ ,<sup>23</sup>  $\Delta V^* \approx 13.0 \text{ \AA}^3$ ,<sup>25</sup> and the volume per molar is about 1% decreased after crystallization from amorphous phase.<sup>24</sup> The data of  $D$ ,  $Q$  ( $\sim 1.0$  eV) are obtained from Ref. 26. The nucleation and growth rates at ambient and HP were estimated from the above equations and parameters and are shown in Fig. 4. At ambient pressure, the  $U_{\max}$  (at 985 K) is at a much higher  $T$

than that of  $I_{\max}$  (840 K) [see Fig. 4(a)]. If the effect of quenched in nuclei is taken into account, the difference is even larger. Upon heating, the alloy at first reaches the temperature where the nucleation rate has a maximum, and the formed nuclei are exposed to the maximum growth rate, resulting in a high crystallization rate during further heating. In contrast, upon cooling the alloy from melt, at the temperature where the melt has the maximum growth rate, the alloy has few nucleus sites and low nucleation rate, and the maximum number of nuclei formed at the same temperature experience low growth rate during further cooling, and lead to low crystallization rate. So the pronounced asymmetry in the crystallization results from the different growth rates during cooling and heating. The different crystallization mechanism in the different  $T$  regimes in SL can also be understood from Fig. 4. At high- $T$  scale in SL region, the liquid has large growth rate but very low nucleation rate. So the formation of nuclei mainly determines the crystallization. At low temperature scale, however, the liquid has large nucleation rate but very low growth rate. The growth of the crystals dominates the crystallization process.

Upon HP heating and cooling, the maximum  $T$  for both growth (1180 K) and nucleation (1050 K) rates shift to much high  $T$  [Fig. 4(b)]. Meanwhile, both the  $I$  and  $U$  are significantly decreased as shown in Fig. 4(b).  $D$  decreases with increasing pressure [ $\Delta V^* > 0$ , and  $\partial(\ln D)/\partial P < 0$ ]. At ambient pressure the pressure effect,  $p\Delta V^*$  ( $\sim 10^{-6}$  eV) is negligible compared to temperature effect,  $k_B T = 0.1$  eV/atom when temperature is increased to 800 K from room temperature. However, when pressure reaches GPa level, the  $Q$  is about 0.05 eV/GPa in vit1 and the pressure effect cannot be ignored anymore. Therefore, the nucleation and growth in SL, which is much lower than the maximum temperature of growth and nucleation rates, are very small under HP, and then the crystallization is much easier to be suppressed under HP. HP reduces the asymmetry in crystallization behavior and suppresses crystallization in the SL by shifting the maximum temperatures of growth and nucleation rates to much high temperatures and increasing viscosity of the liquid.

The financial support from the National Science Foundation of China, Grant Nos. 50321101 and 50371097, is appreciated.

\*Corresponding author. Email address: whw@aphy.iphy.ac.cn

- <sup>1</sup>F. Sciortino, W. Kob, and P. Tartaglia, Phys. Rev. Lett. **83**, 3214 (1999).
- <sup>2</sup>A. Scala, F. W. Starr, E. L. Nave, F. Sciortino, and H. E. Stanley, Nature (London) **406**, 166 (2000).
- <sup>3</sup>K. Koga, H. Tanaka, and X. G. Zeng, Nature (London) **408**, 564 (2000).
- <sup>4</sup>A. Inoue, Acta Mater. **48**, 279 (2000).
- <sup>5</sup>W. L. Johnson, MRS Bull. **24**, 42 (1999); W. H. Wang, C. Dong, and C. H. Shek, Mater. Sci. Eng., R. **44**, 45 (2004).
- <sup>6</sup>J. Schroers, Y. Wu, R. Busch, and W. L. Johnson, Acta Mater. **49**, 2773 (2001).
- <sup>7</sup>C. T. Liu, M. F. Chisholm, and M. K. Miller, Intermetallics **10**, 1105 (2002).
- <sup>8</sup>K. F. Kelton, G. W. Lee, A. K. Gangopadhyay, R. W. Hyers, T. J. Rathz, J. R. Rogers, M. B. Robinson, and D. S. Robinson, Phys. Rev. Lett. **90**, 195504 (2003).
- <sup>9</sup>R. Busch, A. Masuhr, and W. L. Johnson, Mater. Sci. Forum **269-272**, 547 (1988).
- <sup>10</sup>T. Waniuk, J. Schroers, and W. L. Johnson, Phys. Rev. B **67**, 184203 (2003).
- <sup>11</sup>T. Iida and R. I. L. Guthrie, *The Physical Properties of Liquid Metals* (Clarendon, Oxford, 1988).
- <sup>12</sup>J. Schroers, A. Masuhr, W. L. Johnson, and R. Busch, Phys. Rev. B **60**, 11 855 (1999).
- <sup>13</sup>W. H. Wang, D. W. He, D. Q. Zhao, and Y. S. Yao, Appl. Phys. Lett. **75**, 2770 (1999).

- <sup>14</sup>W. H. Wang, Y. X. Zhuang, M. X. Pan, and Y. S. Yao, J. Appl. Phys. **88**, 3914 (2000).
- <sup>15</sup>M. Paluch, R. Casalini, and C. M. Roland, Phys. Rev. B **66**, 092202 (2002).
- <sup>16</sup>Z. Y. Shen, G. Y. Chen, Y. Zhang, and X. J. Yin, Phys. Rev. B **39**, 2714 (1989).
- <sup>17</sup>W. Utsumi, K. Funakoshi, S. Urakawa, M. Yamakata, K. Tsuji, H. Konishi, and O. Shimomura, Rev. High Pressure Sci. Technol. **7**, 1484 (1998).
- <sup>18</sup>A. Mssuhr, T. A. Waniuk, R. Busch, and W. L. Johnson, Phys. Rev. Lett. **82**, 2290 (1999).
- <sup>19</sup>A. L. Greer, Science **267**, 1947 (1995).
- <sup>20</sup>W. H. Wang, R. J. Wang, M. X. Pan, and Y. S. Yao, Appl. Phys. Lett. **79**, 1106 (2001).
- <sup>21</sup>D. Turnbull, Prog. Solid State Phys. **3**, 225 (1956).
- <sup>22</sup>R. Busch, Y. J. Lim, and W. L. Johnson, J. Appl. Phys. **77**, 4039 (1995).
- <sup>23</sup>D. R. Uhlmann, J. F. Heys, and D. Turnbull, Phys. Chem. Glasses **7**, 159 (1966).
- <sup>24</sup>W. H. Wang, L. L. Li, M. X. Pan, and R. J. Wang, Phys. Rev. B **63**, 052204 (2001).
- <sup>25</sup>P. Wen, W. H. Wang, Y. H. Zhao, M. X. Pan, D. Q. Zhao, F. Y. Li, and C. Q. Jin, Phys. Rev. B **69**, 092201 (2004).
- <sup>26</sup>F. Faupel, W. Frank, M-P. Macht, H. Mehrer, V. Naundorf, K. Rätzke, H. R. Schober, S. K. Sharma, and H. Teichler, Rev. Mod. Phys. **75**, 237 (2003).